

Lower order and higher order entanglement in $87\text{Rb } 5S - 5P - 5D$ hyperfine manifold modeled as a four-wave mixing process

Moumita Das¹, Biswajit Sen², Ayan Ray³ and Anirban Pathak⁴

¹*Department of Physics, Siliguri College, Siliguri - 734 001, India*

²*Department of Physics, Vidyasagar Teachers' Training College, Midnapore - 721 101, India*

³*Radiative ion beam facility group, Variable energy cyclotron centre, 1/AF, Bidhan Nagar, Kolkata-700 064, India*

⁴*Jaypee Institute of Information Technology, A 10, Sector 62, Noida, UP 201307, India*

Possibilities of generation of lower order and higher order intermodal entanglement in $87\text{Rb } 5S - 5P - 5D$ hyperfine manifold are rigorously investigated using the Sen-Mandal perturbative technique by showing the equivalence of the system with the four-wave mixing (FWM) process. The investigation has revealed that for a set of experimentally realizable parameters we can observe lower order and higher order intermodal entanglement between pump and signal modes and signal and idler modes in a FWM process associated with the $87\text{Rb } 5S - 5P - 5D$ hyperfine manifold. In addition, trimodal entanglement involving pump, signal and idler modes is also reported.

PACS numbers: 03.65.Ud, 42.65.Hw, 42.50.-p, 42.50.Ar, 42.65.Lm

Keywords: entanglement, four-wave mixing process, higher order nonclassicality, hyperfine manifold of Rb

I. INTRODUCTION

The phenomenon of entanglement has drawn considerable attention since its inception in Einstein, Podolsky and Rosen's (EPR) thought experiment [1]. Entanglement describes a system of particles that have one or more highly correlated quantum properties, such as position, momentum, spin, etc. Specifically, two sub-systems that are entangled cannot be described by independent wavefunctions. Instead the quantum state of the combined system is described by a single wavefunction. For example, in the initial experiments on entanglement conducted with optical parametric amplifier (OPA) [2], a linear intensity dependence was observed in the coincident absorption probability. This has been explained [2–5] by considering the absorption of the signal photon together with the absorption of the idler counterpart, as they “travel” together. This explanation is based on the correlated nature of two photon state, though the usual quadratic dependence signature for a two-photon absorption process is absent in the observation. However, this is simple enough and deficient as it neither distinguishes between the classical correlation and entanglement, nor does it say anything about the higher order entanglement. Later, first part of the deficiency was qualitatively addressed in Ref. [6]. Here, the time asymmetry, which is intrinsic to the two-photon state vector produced by successive decay of a three-level cascade system, is held responsible for the distinction between classical correlation and entanglement. Still the order of entanglement obtainable from a cascade system remains unanswered. In this paper, we have attempted to address this problem by taking recourse to four wave mixing (FWM) process in a cascade system. The FWM process intrinsically acts as a generator of nonclassical states, especially as a generator of entangled photons [7] and offers a unique scope for analyzing the existence of different orders of intermodal entanglement. In the quantum description of the FWM process, simultaneous annihilation of two pump photons (which may have different frequencies) creates a signal-

idler photon pair.

Nonclassical properties associated with the FWM process have been studied almost since the inception of quantum optics. In fact, squeezed light was first experimentally generated using FWM [8]. In the last few decades, nonclassical properties associated with FWM process have been studied in various ways ([9–11] and references therein). Applications of FWM have also been reported in various contexts ([9–15] and references therein). Specifically, applications of FWM have been reported for optical parametric oscillators (OPOs) [9], frequency-comb sources [10], single photon sources for quantum cryptography [10, 12, 13], stimulated generation of superluminal light pulses [11], optical filtering [14], low noise chip-based frequency converter [15], etc. Further, in silicon nanophotonic waveguides, several useful optical phenomena related to telecom-band ($\lambda \approx 1550 \text{ nm}$) all-optical functions (such as, wavelength conversion, signal regeneration and tunable optical delay) have been demonstrated using FWM (see [16] and references therein). In addition to these, FWM has recently been used to develop FWM microscopy [17], which is found to be very useful for the study of the nonlinear optical response of nanostructures [17]; enhancement of FWM (i.e., larger value of third order susceptibility $\chi^{(3)}$ in comparison to existing optical materials) has been observed in plasmonic nanocluster [18].

Thus, we may comment that FWM is an extremely important process, which acts as a test bed for studying non-classicality of photons [9–11]. This fact and the above mentioned applications have motivated us to investigate a particular aspect of FWM for a cascade system: intermodal entanglement. Specifically, in this paper, we investigate the possibilities of generation of lower order and higher order entanglement in FWM process associated with a cascade system because entanglement has been established as one of the most important resource for quantum information processing and quantum communication [19]. To be precise, with the advent of quantum information theory, several interesting phenomena

(e.g., quantum teleportation [20], dense coding [21], etc.) are reported which do not have any classical analogue and which require entanglement as an essential resource. Consequently, several systems have already been investigated as sources of entanglement (see [22, 23] and references therein). However, it is still interesting to find experimentally realizable simple systems that can produce entanglement. In what follows, we will show that FWM process associated with a cascade system can provide us one such experimentally realizable and relatively simple system. It would be apt to note that some efforts have already been made to investigate the existence of intermodal entanglement in FWM process, both theoretically and experimentally ([24–28] and references therein). However, to the best of our knowledge, higher order entanglement is not studied in any of the existing works. Although, studies on higher order nonclassicalities [29–34] have become relevant in the recent past. These works showed that there is indeed a dire necessity to introduce a higher order nonclassical criterion to detect weak nonclassicalities in a relatively easy manner. Keeping these facts in mind, in the present paper, we investigate the possibilities of observing lower order and higher order intermodal entanglement in FWM process associated with a cascade system under the framework of Sen-Mandal perturbative approach [35] that is known to provide analytic expressions for time evolution of field operators with greater accuracy compared to the traditionally used short-time solution [36]. This is well established in earlier works ([23, 37–40] and references therein). In what follows, we report a perturbative solution (using the Sen-Mandal approach) for the Heisenberg's equations of motion for various modes present in the Hamiltonian of the FWM process. The perturbative solution obtained here is subsequently used to investigate the existence of lower order and higher order entanglement using a set of inequalities that can be expressed as moments of annihilation and creation operators. To be precise, we have used here Duan et al.'s criterion [41] and Hillery Zubairy's criteria [42–44] to investigate the existence of intermodal entanglement. The investigation has revealed the signatures of the existence of lower order and higher order intermodal (two-mode) entanglement for all possible combinations of modes (i.e., entanglement is observed between (i) pump and idler modes, (ii) pump and signal modes, (iii) idler and signal modes). Not only that the possibility trimodal entanglement is also investigated here, and it is found that the appropriate choice of parameters yields trimodal entanglement involving pump, signal and idler modes. Remaining part of the paper is organized as follows. In Section II, we describe the relevance of using the $87Rb$ $5S - 5P - 5D$ hyperfine manifold as a test bed for entanglement study by exercising FWM. The model Hamiltonian for the FWM process described in Section II, is described in Section III. This takes into consideration all the four modes as weak and thus quantum mechanical and subsequently we report an operator solution of the Heisenberg's equations of motion corresponding to the each mode of FWM process. The solution is obtained using the Sen-Mandal perturbative approach. In Section IV, possibilities of generation of lower order and higher order (including tri-modal entanglement) in FWM process are studied using the operator so-

lutions obtained in Section III. Finally, the paper is concluded in Section V.

II. THE CASCADE LEVEL COUPLING SCHEME AS TEST BED FOR ENTANGLEMENT

A practical level scheme, where cascade decay can be observed, is $87Rb$ $5S_{\frac{1}{2}} \leftarrow 6P_{\frac{3}{2}} \leftarrow 5D_{\frac{5}{2}}$ route (cf. Fig. 1 a). The excitation of atoms to $5D_{\frac{5}{2}}$ can be done in a two photon process either through an intermediate state, i.e., (I) $5S_{\frac{1}{2}} \xrightarrow{780nm} 5P_{\frac{3}{2}} \xrightarrow{776nm} 5D_{\frac{5}{2}}$ [45] or through (II) a virtual level by using photons of $778nm$ wavelength [46]. However (I) is a more practised option to populate $5D_{\frac{5}{2}}$ as for (II) the absorption cross-section is much smaller. Option (I) is used to describe several important optical processes, e.g., FWM [47], electromagnetically induced transparency (EIT) [48], double resonance optical pumping (DROP) [49], optical switching [50], etc. Fig. 1 illustrates the level scheme under consideration where both (I) and (II) pathways are clearly shown. The life times (τ) are in order: $\tau_{5P_{\frac{3}{2}}}(26ns) < \tau_{6P_{\frac{3}{2}}}(112ns) < \tau_{5D_{\frac{5}{2}}}(240ns)$. Hence $6P_{\frac{3}{2}}$ acts as a leaky reservoir $|r_l\rangle$ w.r.t., $5P_{\frac{5}{2}}$ with a leakage rate slow enough to satisfy $\tau_{6P_{\frac{3}{2}}} \sim \tau_{5P_{\frac{3}{2}}}$. So faster optical pumping and decay cycles centered on $5P_{\frac{3}{2}}$ can be averaged over a single $\tau_{6P_{\frac{3}{2}}}$. This does not violate the steady state condition; further $|r_l\rangle$ is decoupled from the main system. So it bears negligible influence on cascade excitations. On the other hand, $\tau_{6P_{\frac{3}{2}}} \sim 0.5\tau_{5P_{\frac{3}{2}}}$; hence spontaneous decay $5S_{\frac{1}{2}} \leftarrow 6P_{\frac{3}{2}} \leftarrow 5D_{\frac{5}{2}}$ would replicate hyperfine structure of $5D_{\frac{5}{2}}$ level (cf. Fig. 1 a). Similarly, Fig. 1 b illustrates a typical experimental spectrum obtained under pump-probe Rabi frequency combination of $\Omega_{pu}(\Omega_{pr}) \sim 2\pi \times 80MHz(2\pi \times 2MHz)$. Both lasers are plane polarized and satisfy the $5S_{\frac{1}{2}}(F = 2) \xrightarrow{\text{Probe}} 5P_{\frac{3}{2}}(F' = 3) \xrightarrow{\text{Pump}} 5D_{\frac{5}{2}}(F'')$ connection. The X-axis of Fig. 1 b (ii) is calibrated with the saturation absorption spectrum of the probe laser (inset; Fig. 1 b (i)). Here the probe laser is scanned and the pump is stationary. The spectrum shows prominent signatures of DROP [49, 50] on the Doppler broadened background of probe absorption. This situation is further clarified when the probe is locked to $F = 2 \rightarrow F' = 3$ and pump is scanned and blue fluorescence of $5S_{\frac{1}{2}}(F = 2) \xleftarrow{420nm} 5P_{\frac{3}{2}}(F' = 3) \xleftarrow{5.23\mu m} 5D_{\frac{5}{2}}(F'')$ the decay channel is simultaneously monitored (see Fig. 1 b (iii), (iv)). In cases of Fig. 1 b (ii), (iv) the I, II, III represent DROP signals of $F = 2 \rightarrow F'' = 4, 3, 2$ two photon transitions. Unlike Fig. 1 b (ii), the spectrum in (iv) has no Doppler background. Here the locked probe laser in principle addresses small velocity groups of atoms resonant with the same. These atoms further reach $|3\rangle$ by the pump laser itself. Due to participation of highly selective velocity groups of atoms the resultant Doppler background is largely reduced. Though the counter propagating pump-probe combination is favorable for observing strong EIT under two photon resonance ($F = 2 \rightarrow F' =$

$3 \rightarrow F''$) condition (i.e., $\Delta_{pu} + \Delta_{pr} \approx 0$ and $\Delta_{pu} \approx 0 \approx \Delta_{pr}$); only trace of EIT is observed to be present at the tip of DROP profiles. This may be explained by considering the decay route $F = 2 \xleftarrow{\text{branching ratio } (\eta=1)} F' = 3 \xleftarrow{\eta=0.76} F''$, which forms a pseudo-closed absorption-emission cycle. However, due to velocity selective nature (considering $\sqrt{\Omega^2 + \Delta^2}$ is the generalized Rabi frequency where, Δ is laser detuning) of optical pumping, it is apparent that there are also other decay routes, which remain active, resulting in a sufficient population of $F = 1$ state facilitating DROP condition [51] and the EIT is almost obscured. The striking feature of Fig. 1B (iii), i.e. the blue fluorescence, is its one-to-one correspondence with the two photon absorption. This is because blue photons mainly originate from $5S_{1/2} \xleftarrow{\eta=0.23} 6P_{3/2} \xleftarrow{\eta=0.26} F''$ [52] decay channel. In a simplistic manner we may think that under relatively higher pump power ($I_{\text{pump}} \geq I_{\text{saturation } 5P_{3/2} \rightarrow 5D_{5/2}}$) and relatively lower probe power ($I_{\text{probe}} \leq I_{\text{saturation } 5S_{1/2} \rightarrow 5P_{3/2}}$), the blue light intensity (I_{Blue}) bears a correlation of $I_{\text{Blue}} \propto I_{\text{probe}}$. It shows that there exists finite possibility to produce spontaneous emission in a cascade decay, which at least remain intensity correlated to the probe. This intrinsic capability of cascade emission deserves further attention to explore if any kind of phase correlation is obtainable. To generate phase correlation, the co-propagating pump-probe configuration holds edge over the counter-propagating one. This is because FWM is realizable under the first kind of alignment where the phase matching condition demands: $\vec{k}_{780nm} + \vec{k}_{776nm} = \vec{k}_{5.2\mu m} + \vec{k}_{420nm}$. This indeed offers an unique scope where the phase and intensity correlation can be simultaneously obtained. By definition, two beams of light can be made quantum mechanically entangled through correlations of their phase and intensity fluctuations. Hence the cascade system under co-propagating laser action may act as a source of non-classical light.

For a two photon cascade decay ($|3\rangle \rightarrow |2\rangle \rightarrow |1\rangle$) the situation may be understood as follows: (i) initially the atom occupies highest excited state $|3\rangle$ while the field remains in vacuum $|0\rangle$, (ii) the excited atom decays to intermediate state $|2\rangle$ by emitting a photon and makes a final dash to $|1\rangle$ with emission of another photon. To consider the total process, it is not possible to distinguish between the photon emission sequences like $|3\rangle \rightarrow |2\rangle$ followed by $|2\rangle \rightarrow |1\rangle$ or vice versa. In such situation, indistinguishability of photon comes into play. For a cascade system, the product state for (i) is $|3; 0\rangle = |3\rangle |0\rangle$ while for (ii) they are $|2; 1_{\vec{k}s}\rangle = |2\rangle |1_{\vec{k}s}\rangle$ and $|1; 1_{\vec{k}s}, 1_{\vec{k}'s}\rangle = |1\rangle |1_{\vec{k}s}, 1_{\vec{k}'s}\rangle$. The total state vector becomes a linear superposition of these individual state vectors. At the very beginning the atom and the field remains entangled. But at later times the decoherence of the excited level population destroys the entanglement. As a result the final product state appears as: $|3; 1_{\vec{k}s}, 1_{\vec{k}'s}\rangle = |3\rangle |1_{\vec{k}s}, 1_{\vec{k}'s}\rangle$. In this case

$|1_{\vec{k}s}, 1_{\vec{k}'s}\rangle$, which is a two photon state, may be considered to be an entangled state if it is not separable (i.e., $\vec{k}s \neq \vec{k}'s'$); where are wave vector (polarization) of radiation. For a cascade medium the degree of entanglement is determined by the ratio of linewidths of upper and intermediate excited states [6, 53]. Since in the cascade emission of Fig. 1 a $\tau_{5D} > \tau_{6P}$; it is in principle possible to generate entangled light through non-degenerate FWM process.

III. THE MODEL HAMILTONIAN

The quantum mechanical Hamiltonian for FWM process shown in Fig. 1 is

$$H = \omega_a a^\dagger a + \omega_b b^\dagger b + \omega_c c^\dagger c + g (a^2 b^\dagger c^\dagger + a^\dagger b c), \quad (1)$$

where g is the interaction constant and the $a(a^\dagger)$, $b(b^\dagger)$ and $c(c^\dagger)$ are annihilation (creation) operators for two degenerate pump modes, signal mode and idler mode, respectively. Now from the Fig. 1 a, $|1\rangle - |3\rangle$ is populated using two-photon process with the pump mode a and the transition from $|3\rangle$ to $6P_{3/2}$ represents the mode b of the Hamiltonian (1). Finally, mode c corresponds to the transition from $6P_{3/2}$ to $5S_{1/2}$. Here we consider all the modes as weak and that requires a completely quantum mechanical treatment. To obtain the time evolution of the annihilation operators of different modes, we first obtain the Heisenberg's equations of motion for various field operators as

$$\begin{aligned} \dot{a}(t) &= -i(\omega_a a + 2ga^\dagger bc) \\ \dot{b}(t) &= -i(\omega_b b + ga^2 c^\dagger) \\ \dot{c}(t) &= -i(\omega_c c + ga^2 b^\dagger) \end{aligned} \quad (2)$$

These equations are coupled, nonlinear differential equations of field operators and are not exactly solvable in closed analytical forms. Consequently, it is required that we follow a perturbative approach. Here, we have used the Sen-Mandal perturbative technique [23, 35, 40], which is already known to be more general than the well-known short-time approximation approach [36]. Now, following Sen-Mandal's perturbative technique, we can write assumed solutions (assumed analytic forms of the the time evolution of annihilation operators of various modes) as

$$\begin{aligned} a(t) &= f_1 a + f_2 a^\dagger bc + f_3 a b^\dagger b c^\dagger + f_4 a^\dagger a^2 c^\dagger + f_5 a^\dagger a^2 b b^\dagger, \\ b(t) &= g_1 b + g_2 a^2 c^\dagger + g_3 a^2 a^\dagger b + g_4 a^\dagger a b c c^\dagger + g_5 a a^\dagger b c c^\dagger, \\ c(t) &= h_1 c + h_2 a^2 b^\dagger + h_3 a^2 a^\dagger c + h_4 a^\dagger a c b b^\dagger + h_5 a a^\dagger c b b^\dagger, \end{aligned} \quad (3)$$

where f_i, g_i and h_i s are time dependent parameters.

The above mentioned assumed solution is obtained by using the fact that the time evolution of the annihilation operator

$a(t)$ under Hamiltonian H can be expressed as

$$a(t) = \exp(iHt) a(0) \exp(-iHt), \quad (4)$$

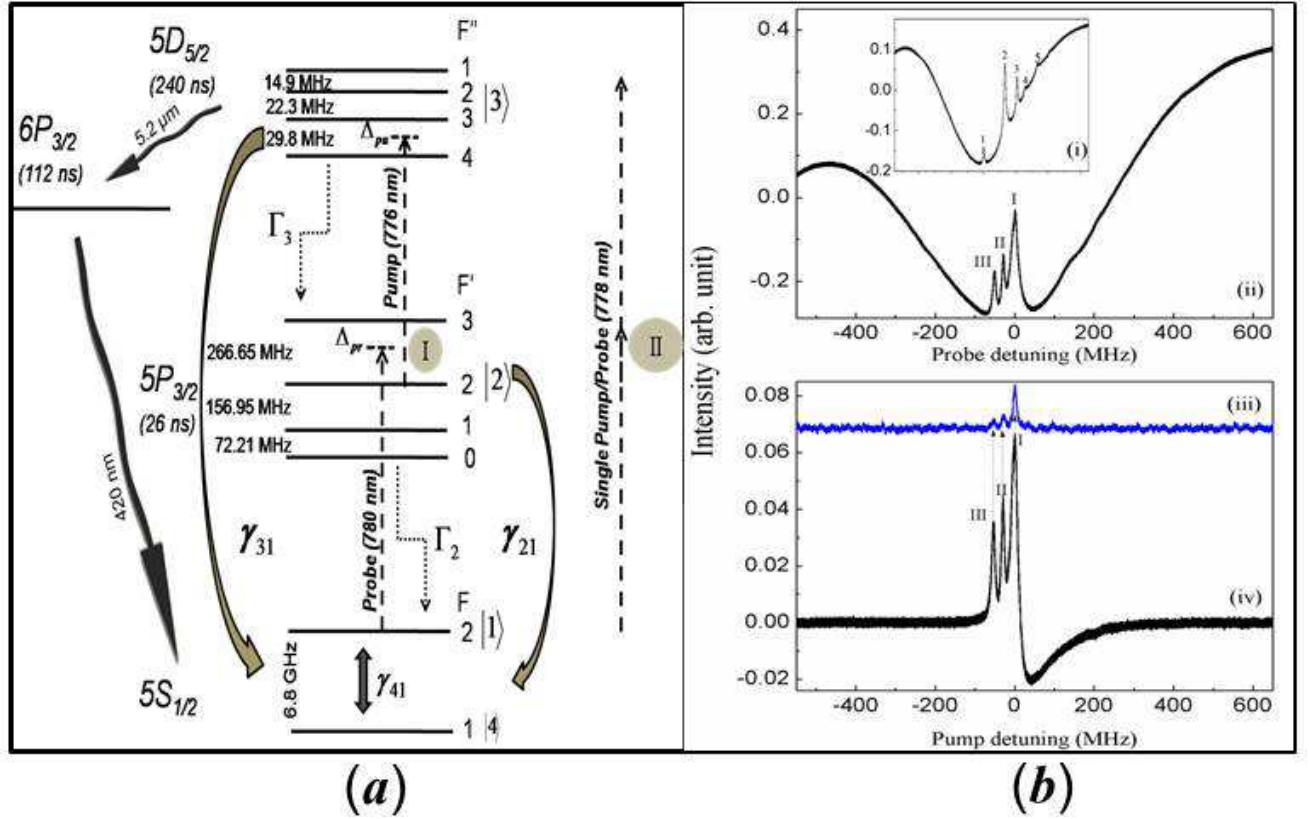


Figure 1: (Color online) Level scheme with result for counter propagating wave. **(a)** Level scheme in $5S_{1/2} \rightarrow 5P_{3/2}(D_2) \rightarrow 5D_{5/2}$ transition (I) of Rubidium atom (^{87}Rb), relevant for DROP (EIT) experiments. The pump (probe) laser beams are linearly polarized. Dephasing between ground state ($|1\rangle$) hyperfine components ($F = 2, 1$) is $\gamma_{g, 1 \leftrightarrow 4}$, governed by the transit time broadening. Spontaneous decay rate from $|j\rangle$ is Γ_j (dotted arrows). Here, $\Gamma_3 = 2\pi \times 0.97 \text{ MHz}$, $\Gamma_2 = 2\pi \times 6.066 \text{ MHz}$, $\Gamma_1 = 0$ are the natural linewidths. The coherent dephasing rate $|j\rangle \rightarrow |i\rangle$ is $\gamma_{ji} \approx (\Gamma_j + \Gamma_i)/2$. The decay route $5S_{1/2} \rightarrow 6P_{3/2}$ {lifetime $\sim 112 \text{ ns}$ } $\leftarrow 5D_{5/2}$ is used to monitor population history at $5D_{5/2}$. Lifetimes of other states are also mentioned below respective level captions. The direct excitation $5S_{1/2} \rightarrow 5D_{5/2}$ (II) is also possible through virtual level. **(b)** Here, the saturation absorption spectrum (i) of Rb is shown where 1,4,5 correspond to $F = 2 \rightarrow F' = 3, 2, 1$ hyperfine components, whereas 2,3 correspond to crossover transitions $F = 2 \rightarrow F' = 3, 2$ and $3, 1$. The DROP spectra $F = 2 \rightarrow F'' = 4, 3, 2$ are presented under (ii) probe laser frequency scan (pump stationary) with Doppler background and (iv) pump laser detuning (probe static) without Doppler background. The plot in (iii) presents the blue fluorescence spectra mimicking the hyperfine separation of $5D_{5/2}$ state.

and the same (i.e., Eq. (4)), can be expanded as

$$a(t) = a(0) + it[H, a(0)] + \frac{(it)^2}{2!}[H, [H, a(0)]] + \frac{(it)^3}{3!}[H, [H, [H, a(0)]]] + \dots \quad (5)$$

It is to be noted that we have neglected the terms beyond g^2 , but have not imposed any restriction on time t provided $gt \ll 1$. Specifically, the assumed solution is obtained by keeping all the terms that arise from the infinite series (5), provided that the terms are not of higher power (higher than quadratic) in g . Subsequently, the assumed solution for a specific mode is substituted in the Heisenberg's equation of motion for that particular mode which is obtained using the given Hamiltonian. Now, the coefficients of the similar terms are compared to obtain a set of coupled ordinary differential equations involving f_i , g_i , and h_i . Finally, this set of coupled differential equations is solved to obtain the final analytic solution. This process leads to some additional terms that are not obtained in the conventional short-time solution. These extra

terms provide an edge to the Sen-Mandal method in comparison to the conventional short-time method. Now, following the prescription described above in general and using Eqns. (2) and (3) in particular, we can obtain the functional forms of these parameters as

$$\begin{aligned} f_1 &= e^{-i\omega_a t} \\ f_2 &= \frac{2g}{\Delta\omega_1} f_1 (1 - e^{i\Delta\omega_1 t}) \\ f_3 &= \frac{2g}{\Delta\omega_1} (f_2 + i2gt f_1) \\ f_5 &= f_4 = -\frac{f_3}{2} \end{aligned} \quad (6)$$

$$\begin{aligned} g_1 &= e^{-i\omega_b t} \\ g_2 &= -\frac{g}{\Delta\omega_1} g_1 (1 - e^{-i\Delta\omega_1 t}) \\ g_3 &= -\frac{g}{\Delta\omega_1} (g_2 + i g t g_1) \\ g_5 &= g_4 = -2g_3 \end{aligned} \quad (7)$$

$$\begin{aligned}
h_1 &= e^{-i\omega_c t} \\
h_2 &= -\frac{g}{\Delta\omega_1} h_1 (1 - e^{-i\Delta\omega_1 t}) \\
h_3 &= -\frac{g}{\Delta\omega_1} (h_2 + i g t h_1) \\
h_5 &= h_4 = -2h_3,
\end{aligned} \tag{8}$$

where $\Delta\omega_1 = 2\omega_a - \omega_b - \omega_c$. Thus, we obtain a perturbative solution for the equations of motion corresponding to the Hamiltonian of the FWM process. The correctness of the above solutions can be checked by the equal time commutation relation (ETCR) i.e., by verifying that $[a(t), a^\dagger(t)] = [b(t), b^\dagger(t)] = [b(t), b^\dagger(t)] = 1$. The obtained solutions may now be used to investigate the existence of lower order and higher order entanglement involving various modes by using a set of moment-based criteria of entanglement. The same is done in the following section.

IV. INTERMODAL ENTANGLEMENT

We have already mentioned that entanglement plays very crucial role in quantum information processing. There exist several inseparability criteria [41–44, 54] which may be used to investigate the possibility of the existence of entanglement in the physical systems. Many of these inseparability criteria (e.g., Hillery and Zubairy's criteria [42–44], Duan et al.'s criterion [41], etc.) are moment based (i.e., they are expressed in terms moments of the annihilation and creation operators of two or more modes), and thus suitable for the present study as we already have closed form analytic expressions for the time evolution of various modes. Interestingly, most of these inseparability criteria are only sufficient and not necessary. Thus, if inseparability condition is found to satisfy, we know with certainty that the investigated state is entangled, but if the condition is not satisfied we cannot conclude anything about the separability. Keeping this in mind, we usually investigate the existence of entanglement using two or more inseparability criteria, so that if one criterion fails to detect entanglement for a specific state and specific parameters, the other criterion (criteria) may succeed to detect it. In what follows, we will use two criteria of Hillery and Zubairy and one criterion of Duan et al. Further, we would like to note that these inseparability criteria can be classified as: (i) Lower order criteria: If an inseparability criterion (inequality) contains terms only up to fourth order in the annihilation and/or creation operators of different modes, the criterion is referred to as a lower order criterion. This is so, as to study the correlations between two modes we need at least fourth order terms. Consequently, all criteria that involve terms up to 4th order in annihilation/creation operators are known as lower order criteria. (ii) Higher order criteria: If an inseparability criterion (inequality) contain terms of order higher than the fourth order in the annihilation and/or creation operators of different modes, the criterion is referred to as a higher order criterion. We can easily see that by this definition all inseparability criteria for three or more modes (or involving three or more particles) must be higher order criteria. Interestingly, one can also construct higher order criteria for the investigation of entanglement in two-mode case [42, 54]. In what follows, we will

study higher order entanglement from both the perspectives (i.e., three-mode cases and two mode higher order cases), but to begin with, in the next subsection we investigate the possibility of observing lower order entanglement between two modes of FWM process.

To investigate the possibilities of observing entanglement in FWM process, we consider that the initial state $|\psi(0)\rangle$ is separable and is the product of three coherent states corresponding to three modes of the system. Further, we assume that $|\alpha|^2$, $|\beta|^2$ and $|\gamma|^2$ are the initial number of photons in each pump mode, signal mode and idler mode, respectively. Thus, we have

$$|\psi(0)\rangle = |\alpha\beta\gamma\rangle = |\alpha\rangle \otimes |\beta\rangle \otimes |\gamma\rangle. \tag{9}$$

A. Lower order two-mode entanglement

To obtain the signature of entanglement in FWM process, we have used the following inseparability criteria introduced by Hillery and Zubairy [42–44]

$$E_{a,b} = \langle N_a N_b \rangle - |\langle ab^\dagger \rangle|^2 < 0 \tag{10}$$

and

$$E'_{a,b} = \langle N_a \rangle \langle N_b \rangle - |\langle ab \rangle|^2 < 0 \tag{11}$$

where a and b represent two arbitrary modes. Throughout our present paper, we refer to these inequalities (10) and (11) as HZ1 and HZ2 criteria, respectively. As these two criteria are only sufficient not necessary, we also use another moment based inseparability criterion which is referred to as Duan et al.'s criterion [41] for any two arbitrary mode a and b , Duan et al.'s criterion describes the condition of inseparability as

$$D_{ab} = (\Delta u)^2 + (\Delta v)^2 - 2 < 0, \tag{12}$$

where

$$\begin{aligned}
u &= \frac{1}{\sqrt{2}} \{ (a + a^\dagger) + (b + b^\dagger) \}, \\
v &= -\frac{i}{\sqrt{2}} \{ (a - a^\dagger) + (b - b^\dagger) \}.
\end{aligned} \tag{13}$$

Now using Eqns. (3), (9) and HZ1 criterion (10), we obtain

$$E_{a,b} = |f_2|^2 \left(\frac{1}{4} |\alpha|^6 + |\beta|^4 |\gamma|^2 - \frac{1}{2} |\alpha|^4 |\beta|^2 - |\alpha|^2 |\beta|^2 |\gamma|^2 \right), \tag{14}$$

$$\begin{aligned}
E_{b,c} &= |g_2|^2 \left[|\alpha|^4 \left(1 + 3 |\beta|^2 + 3 |\gamma|^2 \right) - 2 |\beta|^2 |\gamma|^2 \right. \\
&\quad \times \left. \left(1 + 2 |\alpha|^2 \right) \right] + (h_1 h_2^* \alpha^{*2} \beta \gamma + \text{c.c.})
\end{aligned} \tag{15}$$

$$E_{a,c} = |f_2|^2 \left(\frac{1}{4} |\alpha|^6 + |\beta|^2 |\gamma|^4 - \frac{1}{2} |\alpha|^4 |\gamma|^2 - |\alpha|^2 |\beta|^2 |\gamma|^2 \right), \tag{16}$$

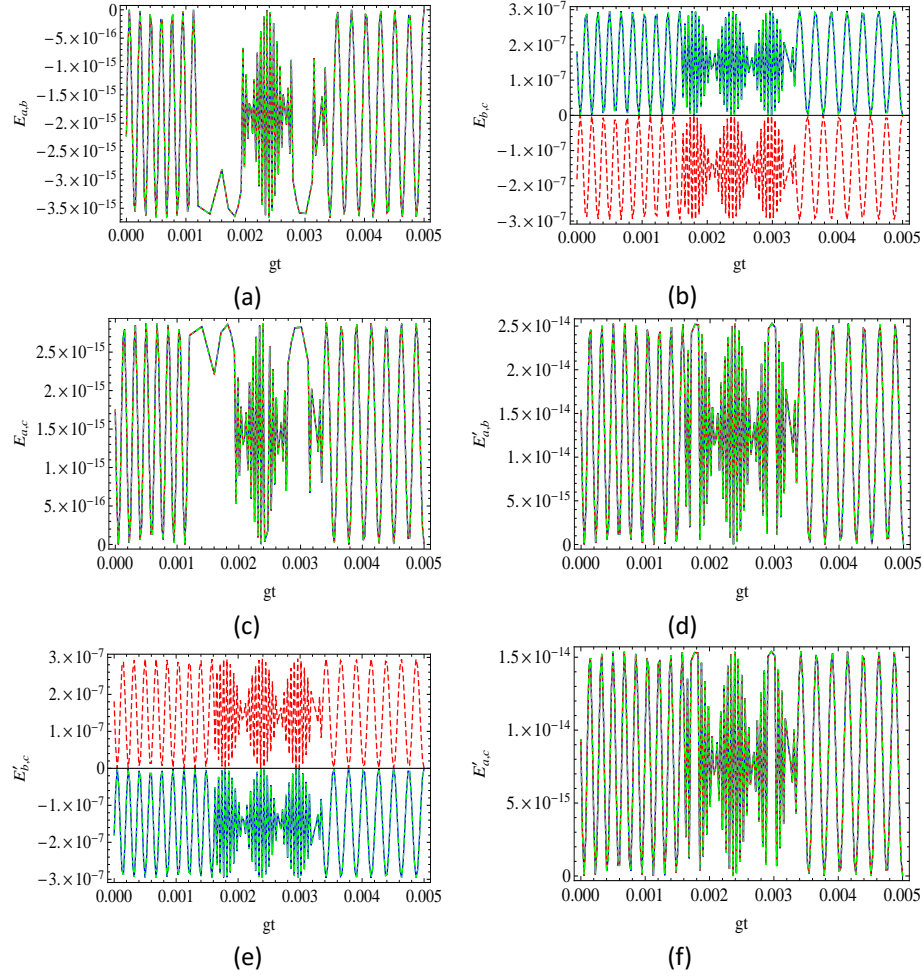


Figure 2: (Color online) Lower order entanglement using HZ1 and HZ2 criteria. The solid (blue), dash-dotted (green), and dashed (red) lines represent the phase angle of the input complex amplitude α_s for $\phi = 0, \pi/2$ and π , respectively, using $\omega_a = 242.38 \times 10^{13}$ Hz, $\omega_b = 36.05 \times 10^{13}$ Hz, $\omega_c = 448.98 \times 10^{13}$ Hz, $\alpha = 5$, $\beta = 4$ and $\gamma = 2$. Intermodal entanglement is observed using HZ1 criterion in the coupled mode: (a) ab mode for all values of the phase angle ϕ , (b) bc mode for $\phi = \frac{\pi}{2}$. No signature of entanglement in (c) ac mode is observed using HZ1 criterion, but using HZ2 criterion, we observed entanglement in (e) bc mode for the phase angle 0 and π only. No signature of inter modal entanglement is observed in (d) ab mode and (e) ac mode using HZ2 criterion.

where we have assumed that the initial state is described by (9). The same initial state is used in the entire paper. Now, we plot right hand sides of (14)-(16) in Fig. 2(a)-(c) with three values of the phase ϕ of input pump mode a . Precisely, we have considered $\alpha = |\alpha| \exp(i\phi)$ and plotted right hand sides of (14)-(16) using $\phi = 0, \frac{\pi}{2}$ and π . Negative regions of the plots clearly illustrate bi-modal entanglement in ab modes for all values ϕ and in bc modes for $\phi = \frac{\pi}{2}$. We could

not find any signature of entanglement for ac mode. However, we cannot conclude anything about the separability/inseparability in those cases where negative regions are not found. This is so because the HZ1 criterion and other similar criteria of inseparability used in this paper are only sufficient and not necessary. Similarly, we may use (3), (9) and (11) to obtain

$$E'_{a,b} = |f_2|^2 \left(\frac{1}{4} |\alpha|^6 + |\beta|^4 |\gamma|^2 + \frac{1}{2} |\alpha|^4 |\beta|^2 + |\alpha|^2 |\beta|^2 |\gamma|^2 \right), \quad (17)$$

$$E'_{b,c} = |g_2|^2 \left[2 |\beta|^2 |\gamma|^2 (1 + 2 |\alpha|^2) - |\alpha|^4 (1 + |\beta|^2 + |\gamma|^2) \right] - (h_1 h_2^* \alpha^{*2} \beta \gamma + c.c.), \quad (18)$$

$$E'_{a,c} = |f_2|^2 \left(\frac{1}{4} |\alpha|^6 + |\beta|^2 |\gamma|^4 + \frac{1}{2} |\alpha|^4 |\gamma|^2 + |\alpha|^2 |\beta|^2 |\gamma|^2 \right). \quad (19)$$

As before, we plot right hand sides of Eqns. (17)-(19) in Figs.2(d)-(f) and it is clear from the figures that the intermodal entanglement is observed only in bc mode for the phase angle $\phi = 0$ and π . No signature of intermodal entanglement is observed in the remaining two cases. As discussed above, in these cases we are nonconclusive about the inseparability.

Now, we may extend our investigation on inseparability using Duan et al.'s criterion described in Eq. (12) and obtain the following expressions with the help of the solutions (3), (6)-(8) described in the previous section:

$$D_{ab} = D_{ac} = |f_2|^2 \left(\frac{1}{2} |\alpha|^4 + 2 |\beta|^2 |\gamma|^2 \right), \quad (20)$$

$$D_{bc} = |f_2|^2 |\alpha|^4, \quad (21)$$

Right hand sides of Eqns. (20) - (21) are clearly positive and thus we may conclude that for the physical system studied

here, Duan et. al.'s criterion cannot identify any signature of entanglement.

B. Higher order entanglement

In order to investigate the existence of bi-modal higher order entanglement in FWM process, we may use the following two criteria introduced by Hillery and Zubairy [42]:

$$\begin{aligned} E_{a,b}^{m,n} &= \langle a^{\dagger m} a^m b^{\dagger n} b^n \rangle - |\langle a^m b^{\dagger n} \rangle|^2 < 0 \\ E_{a,b}'^{m,n} &= \langle a^{\dagger m} a^m \rangle \langle b^{\dagger n} b^n \rangle - |\langle a^m b^n \rangle|^2 < 0, \end{aligned} \quad (22)$$

where a and b are two arbitrary modes and m and n are the positive integers. Here, $m + n \geq 3$ gives the criteria for higher order entanglement. The negativity of the right hand side would show the signature of the entanglement. Now, using the first higher order criteria of Hillery and Zubairy for various field modes we obtain

$$\begin{aligned} E_{a,b}^{m,n} &= |f_2|^2 \left[m^2 |\alpha|^{2m-2} |\beta|^{2n+2} |\gamma|^2 + m^2 n |\alpha|^{2m-2} |\beta|^{2n} |\gamma|^2 \right. \\ &\quad - \frac{m^2 n (m+1)}{2} |\alpha|^{2m-2} |\beta|^{2n} |\gamma|^2 - mn |\alpha|^{2m} |\beta|^{2n} |\gamma|^2 \\ &\quad - \frac{mn}{2} |\alpha|^{2m+2} |\beta|^{2n} - \frac{m^2 n (m-1)^2}{4} |\alpha|^{2m-4} |\beta|^{2n} |\gamma|^2 \\ &\quad \left. + \frac{n^2}{4} |\alpha|^{2m+4} |\beta|^{2n-2} - \frac{mn(m-1)}{4} |\alpha|^{2m} |\beta|^{2n} \right], \end{aligned} \quad (23)$$

$$\begin{aligned} E_{b,c}^{m,n} &= |g_2|^2 \left\{ (2mn^2 + n^2) |\alpha|^4 |\beta|^{2m} |\gamma|^{2n-2} + m^2 n^2 |\alpha|^4 |\beta|^{2m-2} |\gamma|^{2n-2} \right. \\ &\quad + (2m^2 n + m^2) |\alpha|^4 |\beta|^{2m-2} |\gamma|^{2n} - 2mn (1 + 2|\alpha|^2) |\beta|^{2m} |\gamma|^{2n} \left. \right\} \\ &\quad + \left[mn \left(h_1 h_2^* \frac{\alpha^2}{\beta^* \gamma^*} + (m-1) \frac{h_2^2}{h_1^2} \frac{\alpha^4 \beta^*}{\beta \gamma^2} \right) |\beta|^{2m} |\gamma|^{2n} + mn (m-1) \frac{h_2^2}{h_1^2} \right. \\ &\quad \left. \times \left(\frac{\alpha^4 \gamma^*}{\beta^2 \gamma} + \frac{(n-1)}{2} \frac{\alpha^4}{\beta^2 \gamma^2} \right) |\beta|^{2m} |\gamma|^{2n} \right] + \text{c.c.}, \end{aligned} \quad (24)$$

and

$$\begin{aligned} E_{a,c}^{m,n} &= |f_2|^2 \left[m^2 |\alpha|^{2m-2} |\gamma|^{2n+2} |\beta|^2 + m^2 n |\alpha|^{2m-2} |\gamma|^{2n} |\beta|^2 \right. \\ &\quad - \frac{m^2 n (m+1)}{2} |\alpha|^{2m-2} |\gamma|^{2n} |\beta|^2 - mn |\alpha|^{2m} |\gamma|^{2n} |\beta|^2 \\ &\quad - \frac{mn}{2} |\alpha|^{2m+2} |\gamma|^{2n} - \frac{m^2 n (m-1)^2}{4} |\alpha|^{2m-4} |\gamma|^{2n} |\beta|^2 \\ &\quad \left. + \frac{n^2}{4} |\alpha|^{2m+4} |\gamma|^{2n-2} - \frac{mn(m-1)}{4} |\alpha|^{2m} |\gamma|^{2n} \right]. \end{aligned} \quad (25)$$

To illustrate the fact that Eqs. (23)-(25) provide us signatures of higher order entanglement, we have plotted the right hand

sides of these equations with the dimensionless interaction time gt , in Fig. 3 a-c, where negative regions of the curves

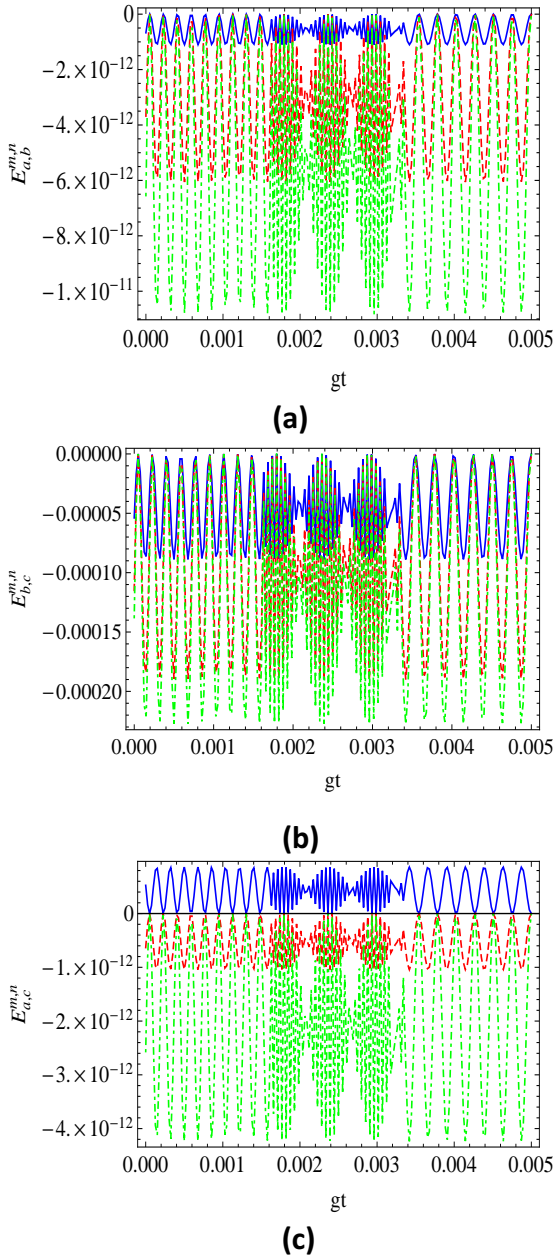


Figure 3: (Color online) Plot of higher order entanglement using HZ1 criterion using $\omega_a = 242.38 \times 10^{13}$ Hz, $\omega_b = 36.05 \times 10^{13}$ Hz, $\omega_c = 448.98 \times 10^{13}$ Hz, $\alpha = 5$, $\beta = 4$ and $\gamma = 2$. The solid (blue) line, dashed (red) line and dash-dotted (green) line represent the $n = 1$, and $m = 1, 2$ and 3 , respectively. Here, in all the plots $n = 1$ and $m = 2$ and 3 are multiplied by 300 and 20 , respectively. Higher order intermodal entanglement is observed in (a) ab mode, (b) bc mode for phase angle $\phi = \frac{\pi}{2}$ and for (c) ac mode.

depict the existence of higher order entanglement. These figure reveal that the signature of the higher order entanglement is observed in all three possible combinations in which two modes can be chosen. Here, in Fig.3, there are three lines in each plot, and they represent three cases for each choice of modes i.e., for $n = 1$ and $m = 1, 2$ and 3

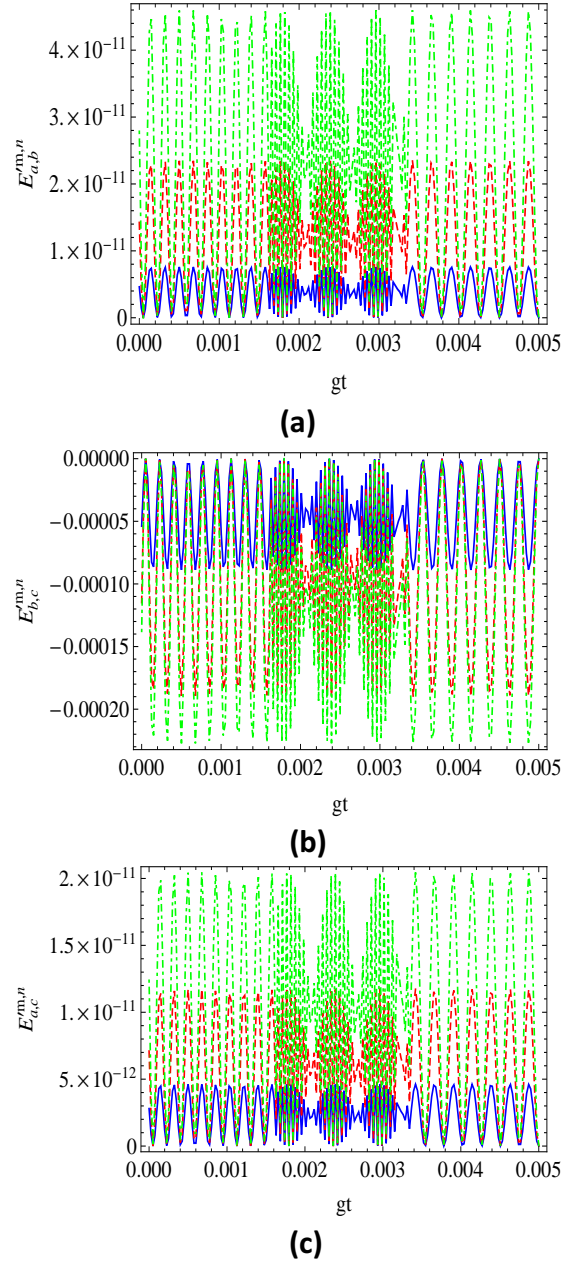


Figure 4: (Color online) Higher order entanglement using HZ2 criterion using $\omega_a = 242.38 \times 10^{13}$ Hz, $\omega_b = 36.05 \times 10^{13}$ Hz, $\omega_c = 448.98 \times 10^{13}$ Hz, $\alpha = 5$, $\beta = 4$ and $\gamma = 2$. The solid (blue), dashed (red), and dash-dotted (green) lines represent $n = 1$ and $m = 1, 2$ and 3 , respectively. Here, in figure, $m = 1$ and $n = 2$ and 3 are multiplied by 300 and 20 , respectively. Higher order intermodal entanglement is observed in (b) bc mode for phase angle 0 and π (not shown) only; but no signature of intermodal entanglement is observed in (a) ab and (c) ac modes.

respectively. Plot for $m = n = 1$ (i.e., blue smooth line) corresponds to normal order entanglement, whereas the $n = 1, m = 2$ (red dashed line) and $n = 1, m = 3$ (green dot dashed line) correspond to the higher order entanglement. It is clear from the figure that the higher order intermodal entanglement is observed for all three modes using HZ1

criterion. Further, Fig.3 c illustrates that for ac modes signature of lower order entanglement is not observed, but that of higher order entanglement is observed. In the similar

manner, using the second criteria of the Hillery-Zubeiry we obtain

$$E_{a,b}^{m,n} = |f_2|^2 \left[m^2 |\alpha|^{2m-2} |\beta|^{2n+2} |\gamma|^2 + \frac{1}{4} mn (m-1) |\alpha|^{2m} |\beta|^{2n} + \frac{mn}{2} |\alpha|^{2m+2} |\beta|^{2n} + \frac{n^2}{4} |\alpha|^{2m+4} |\beta|^{2n-2} + mn |\alpha|^{2m} |\beta|^{2n} |\gamma|^2 \right], \quad (26)$$

$$E_{b,c}^{m,n} = |g_2|^2 \left\{ (m^2 - 2m^2 n) |\alpha|^4 |\beta|^{2m-2} |\gamma|^{2n} - m^2 n^2 |\alpha|^4 |\beta|^{2m-2} |\gamma|^{2n-2} + (1 - 2m) n^2 |\alpha|^4 |\beta|^{2m} |\gamma|^{2n-2} + 2mn (1 + 2|\alpha|^2) |\beta|^{2m} |\gamma|^{2n} \right\} - \left[\left\{ mn \left(h_1 h_2^* \frac{\alpha^{*2}}{\beta^* \gamma^*} + (m-1) \frac{h_2^2}{h_1^2} \frac{\alpha^4 \gamma^*}{\beta^2 \gamma} \right) |\beta|^{2m} |\gamma|^{2n} + mn (n-1) \frac{h_2^2}{h_1^2} \left(\frac{\alpha^4 \beta^*}{\beta \gamma^2} + \frac{(m-1)}{2} \frac{\alpha^4}{\beta^2 \gamma^2} \right) |\beta|^{2m} |\gamma|^{2n} \right\} + \text{c.c.} \right], \quad (27)$$

and

$$E_{a,c}^{m,n} = |f_2|^2 \left[m^2 |\alpha|^{2m-2} |\beta|^2 |\gamma|^{2n+2} + \frac{n^2}{4} |\alpha|^{2m+4} |\gamma|^{2n-2} + \frac{mn}{2} |\alpha|^{2m+2} |\gamma|^{2n} + \frac{mm(m-1)}{4} |\alpha|^{2m} |\gamma|^{2n} + mn |\alpha|^{2m} |\beta|^2 |\gamma|^{2n} \right]. \quad (28)$$

Right hand sides of the above set of equations are plotted in Fig. 4 a-c, which clearly show the signature of the higher order intermodal entanglement for bc mode for the phase angle 0 and π . However, it does not show the same for other choices of modes. Thus, HZ2 criterion could not detect the signature of higher order entanglement in ab and ac mode. In other words, HZ2 criterion fails to detect the higher order intermodal entanglement for ab and ac modes for any phase angle ϕ .

There is another way to investigate the higher order entanglement. Any multi-mode entangled state (which involve more than two modes) is considered to be higher

order entangled. In what follows, we investigate the possibility of observing trimodal entanglement in FWM process using the following criterion [55]

$$E_{a,b,c} = \langle N_a N_b N_c \rangle - |\langle abc^\dagger \rangle|^2 < 0, \quad (29)$$

where a, b, c represents three different modes. Now, we may note that above criterion actually contain three criteria which represent three different bipartite cuts, and we may obtain analytic expressions for $E_{i,j,k}$ for various choices of k mode as follows:

$$E_{a,b,c} = |f_2|^2 \left\{ \frac{1}{4} |\alpha|^6 \left(1 + 3 |\beta|^2 + 3 |\gamma|^2 \right) - \frac{1}{2} |\alpha|^2 |\beta|^2 |\gamma|^2 \times \left(5 |\alpha|^2 + 2 |\beta|^2 + 3 \right) + |\beta|^4 |\gamma|^4 \right\} + \left\{ \left(h_1 h_2^* |\alpha|^2 \alpha^{*2} \beta \gamma + f_1^* f_2 g_1 g_2^* \alpha^{*4} \beta^2 \gamma^2 \right) + \text{c.c.} \right\}, \quad (30)$$

$$E_{b,c,a} = |f_2|^2 \left\{ \frac{1}{4} |\alpha|^6 \left(|\beta|^2 + |\gamma|^2 \right) - \left(1 + |\alpha|^2 + |\beta|^2 + |\gamma|^2 \right) \times |\alpha|^2 |\beta|^2 |\gamma|^2 + |\beta|^4 |\gamma|^4 \right\}, \quad (31)$$

and

$$E_{a,c,b} = |f_2|^2 \left\{ \frac{1}{4} |\alpha|^6 \left(1 + 3 |\beta|^2 + 3 |\gamma|^2 \right) - \frac{1}{2} |\alpha|^2 |\beta|^2 |\gamma|^2 \times \left(5 |\alpha|^2 + 2 |\gamma|^2 + 3 \right) + |\beta|^4 |\gamma|^4 \right\} + \left\{ \left(h_1 h_2^* |\alpha|^2 \alpha^{*2} \beta \gamma + f_1^* f_2 g_1 g_2^* \alpha^{*4} \beta^2 \gamma^2 \right) + \text{c.c.} \right\}. \quad (32)$$

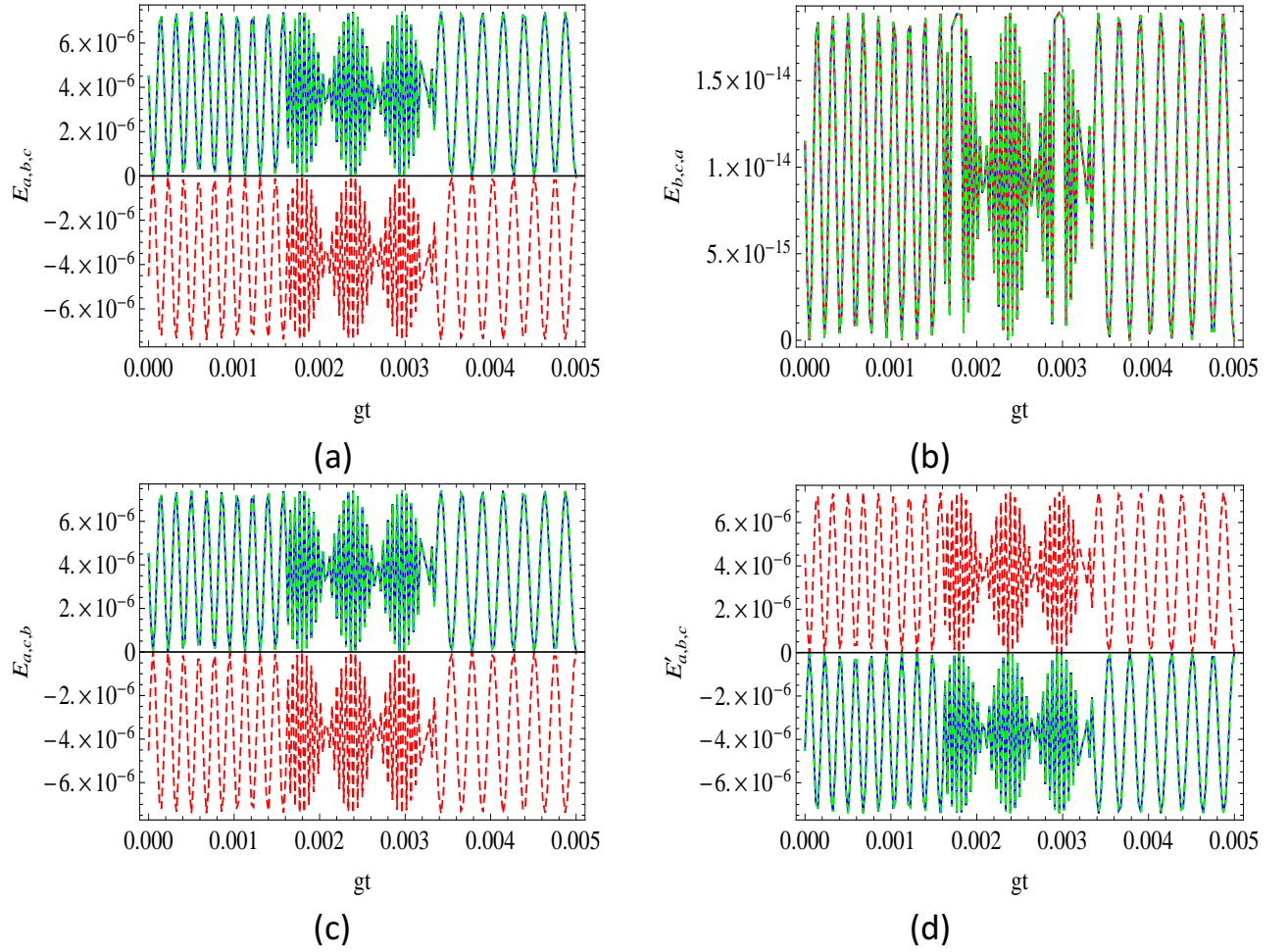


Figure 5: (Color online) Tri-partite entanglement using the HZ1 and HZ2 criteria. The solid (blue), dash-dotted (green) and dashed (red) lines represent the phase angle of the input complex amplitude α_s for $\phi = 0, \pi/2$ and π , respectively, using $\omega_a = 242.38 \times 10^{13}$ Hz, $\omega_b = 36.05 \times 10^{13}$ Hz, $\omega_c = 448.98 \times 10^{13}$ Hz, $\alpha = 5$, $\beta = 4$ and $\gamma = 2$. Trimodal entanglement is observed using HZ1 criterion in (a) abc mode for phase angle $\phi = \frac{\pi}{2}$ (c) acb mode and for the phase angle $\phi = \frac{\pi}{2}$. No signature of entanglement is observed in (c) bca mode. (d) Trimodal entanglement using HZ2 is observed for the phase angle $\phi = 0$ and π only.

If any of the above quantity (i.e., E_{abc} , E_{acb} , E_{bca}) is found to be negative, we will have a signature of trimodal entanglement. To obtain this signature Eqs. (30)-(32) are plotted in Fig. 5 a-c, where we observe negative regions for appropriate choices of phase. This indicates the existence of the trimodal entanglement. To further illustrate the existence of trimodal entanglement involving pump, signal and idler

modes, we further investigate its existence by using a symmetric criterion for inseparability of three modes. The criterion describes the condition for trimodal entanglement as $\langle N_a \rangle \langle N_b \rangle \langle N_c \rangle - |\langle abc \rangle|^2 < 0$ and using Eqs. (3) and (9), we obtain

$$\begin{aligned} \langle N_a \rangle \langle N_b \rangle \langle N_c \rangle - |\langle abc \rangle|^2 &= |f_2|^2 \left\{ -\frac{1}{4} |\alpha|^6 (1 + |\beta|^2 + |\gamma|^2) + |\alpha|^2 |\beta|^2 |\gamma|^2 \right. \\ &\quad \times \left(3 |\alpha|^2 + |\beta|^2 + |\gamma|^2 + \frac{3}{2} \right) + |\beta|^4 |\gamma|^4 \Big\} \\ &\quad - \left\{ \left(h_1 h_2^* |\alpha|^2 \alpha^{*2} \beta \gamma + f_1 f_2^* h_1^* h_2 \alpha^4 \beta^{*2} \gamma^{*2} \right) + \text{c.c.} \right\}. \end{aligned} \quad (33)$$

Variation of RHS of this particular equation is plotted in Fig. 5 d, which also illustrate the possible existence of trimodal

entanglement (for specific choice phase) via its negative

region.

V. CONCLUSION

Traditionally, FWM process is viewed as a third order nonlinear optical phenomenon having applications in various fields as summarized in Sec. I. Recently, the domain of the generation and applicability of FWM have been considerably amplified. Specifically, several new applications of FWM have been proposed. On the other hand, applications of entangled states have been reported in various areas of quantum information. Motivated by these facts, we have rigorously investigated the generation of lower order and higher order intermodal entanglement in FWM process using a set of moment-based criteria (criteria based on moments of annihilation and creation operators) and a physical system illustrated in Fig.1, where FWM happens. To be precise, present discussion is focused on a cascade system shown in Fig.1, where FWM process occurs for $87Rb\ 5S - 5P - 5D$ hyperfine manifold. Considering experimentally achievable

parameters, it's observed that the parameters whose negative values indicate the existence of higher/lower order entanglement show an oscillatory nature with variation of rescaled time. Further, it is observed that suitable choice of the phase of the initial coherent states plays a crucial role in the generation of entanglement. Here, we observed bimodal entanglement between pump and signal modes and signal and idler modes, and have also observed trimodal entanglement using all these modes. Thus, the output of FWM process studied here appears to be highly entangled. We conclude the paper with a hope that this highly entangled output of FWM process would find some applications in quantum communication and/or quantum information processing as FWM is a process that can be easily realized experimentally (cf. Fig.1) and as entanglement is one of the most important resource for quantum communication and computation.

Acknowledgment: AP thanks Department of Science and Technology (DST), India for the support provided through the project number EMR/2015/000393. . The authors also thank Kishore Thapliyal for his interest in the work and some fruitful discussions.

-
- [1] A. Einstein, B. Podolsky, and N. Rosen, Phys. Rev. **47**, 477 (1935).
 - [2] S. Friberg, C. K. Hong, and L. Mandel, Opt. Commun. **54**, 311 (1985).
 - [3] J. Gea-Banacloche, Phys. Rev. Lett. **62**, 1603 (1989).
 - [4] J. Javanainen and P. L. Gould, Phys. Rev. A **41**, 5088 (1990).
 - [5] H. B. Fei et al., Phys. Rev. Lett. **78**, 1679 (1997).
 - [6] A. Muthukrishnan, G.S. Agarwal, and M.O. Scully, Phys. Rev. Lett. **93**, 093002 (2004).
 - [7] V. Boyer, A. M. Marino, R. C. Pooser, and P. D. Lett, Science **321**, 544 (2008).
 - [8] R. Slusher, L. W. Hollberg, B. Yurke, J. C. Mertz, and J. F. Valley, Phys. Rev. Lett. **55**, 2409 (1985).
 - [9] A. Dutt, L. Kevin, S. Manipatruni, A. L. Gaeta, P. Nussenzveig, and M. Lipson. Physical Review Applied **3**, 044005 (2015).
 - [10] C. Reimer, L. Caspani, M. Clerici, M. Ferrera, M. Kues, M. Peccianti, A. Pasquazi, et al, Opt. Express **22**, 6535 (2014).
 - [11] R. T. Glasser, U. Vogl, and P. D. Lett, Phys. Rev. Lett. **108**, 173902 (2012).
 - [12] Y. Wu, M. G. Payne, E. W. Hagley, and L. Deng, Phys. Rev. A **70**, 063812 (2004).
 - [13] M. Fiorentino, P. L. Voss, J. E. Sharping, and P. Kumar. IEEE Photonics Technology Letters, **14**, 983 (2002).
 - [14] D. S. Ding, et al. arXiv:1410.7931 (2014).
 - [15] I. Agha, M. Davanço, B. Thurston, and K. Srinivasan, Optics letters **37**, 2997 (2012).
 - [16] X. Liu, R. M. Osgood, Y. A. Vlasov, and W. M. J. Green, Nature Photonics **4**, 557 (2010).
 - [17] Y. Wang, C. Y. Lin, A. Nikolaenko, V. Raghunathan, and E. O. Potma, Adv. Opt. Photon. **3**, 1 (2011).
 - [18] Y. Zhang, F. Wen, Y. R. Zhen, P. Nordlander, and N. J. Halas, Proceedings of the National Academy of Sciences, **110**, 9215 (2013).
 - [19] A. Pathak, Elements of Quantum Computation and Quantum Communication, CRC Press, Boca Raton, USA (2013).
 - [20] C. H. Bennett, G. Brassard, C. Crepeau, R. Jozsa, A. Peres, and W. K. Wootters, Phys. Rev. Lett. **70**, 1895 (1993).
 - [21] C. H. Bennett and S. J. Wiesner, Phys. Rev. Lett. **69**, 2881 (1992).
 - [22] A. Pathak, J. Křepelka, and J. Peřina, Phys. Let. A **377**, 2692 (2013).
 - [23] B. Sen, S. K. Giri, S. Mandal, C. H. R. Ooi and A. Pathak, Phys. Rev. A **87**, 022325 (2013).
 - [24] Q. Glorieux, R. Dubessy, S. Guibal, L. Guidoni, J. P. Likforman, T. Coudreau, and E. Arimondo, Phys. Rev. A **82**, 033819 (2010).
 - [25] Q. Glorieux, J. B. Clark, N. V. Corzo, and P. D. Lett, New J. Phys. **14**, 123024 (2012).
 - [26] M. G. Payne and L. Deng, Phys. Rev. Lett. **91**, 123602 (2003).
 - [27] Y. Wu, M. G. Payne, E. W. Hagley, and L. Deng, Phys. Rev. A **69** 063803 (2004).
 - [28] Y. B. Yu, J. T. Sheng, and M. Xiao, Phys. Rev. A **83**, 012321 (2011).
 - [29] A. Verma and A. Pathak, Phys. Lett. A **374**, 1009 (2010).
 - [30] A. Pathak and M. Garcia, Applied Physics B **84**, 484 (2006).
 - [31] A. Allevi, S. Olivares, and M. Bondani, Phys. Rev. A **85**, 063835 (2012).
 - [32] A. Allevi, S. Olivares, and M. Bondani, Int. J. Quant. Info. **8**, 1241003 (2012).
 - [33] M. Avenhaus, K. Laiho, M. V. Chekhova, and C. Silberhorn, Phys. Rev. Lett **104**, 063602 (2010).
 - [34] M. Hamar, V. Michálek, and A. Pathak, Measurement Sci. Rev. **14** 227 (2014).
 - [35] B. Sen and S. Mandal, J. Mod. Phys. **52**, 1798 (2005).
 - [36] D. K. Giri and P. S. Gupta, J. Opt. B: Quantum Semiclassical Opt. **6**, 91 (2004).
 - [37] K. Thapliyal, A. Pathak, B. Sen, and J. Peřina, Phys. Rev. A **90**, 013808 (2014).
 - [38] K. Thapliyal, A. Pathak, B. Sen, and J. Peřina, Phys. Lett. A **378**, 3431 (2014).
 - [39] K. Thapliyal, A. Pathak, and J. Peřina, Phys. Rev. A **93**,

- 022107 (2016).
- [40] S. K. Giri, B. Sen, C. H. R. Ooi, and A. Pathak, Phys. Rev. A **89**, 033628 (2014).
 - [41] L. M. Duan, G. Giedke, J. I. Cirac, and P. Zoller, Phys. Rev. Lett. **84**, 2722 (2000).
 - [42] M. Hillery and M. S. Zubairy, Phys. Rev. Lett. **96**, 050503 (2006).
 - [43] M. Hillery and M. S. Zubairy, Phys. Rev. A **74**, 032333 (2006).
 - [44] M. Hillery, H. T. Dung, and H. Zheng, Phys. Rev. A **81**, 062322 (2010).
 - [45] M. B. Kienlen, N. T. Holte, H. A. Dassonville, and A. M. C. Dawes, Am. J. Phys. **81**, 442 (2013).
 - [46] A. J. Olson, E. J. Carlson, and S. K. Mayer, Am. J. Phys. **74**, 218 (2006).
 - [47] A. M. Akulshin, R. J. McLean, A. I. Sidorov, and P. Hannaford, Opt. Exp. **17**, 22861 (2009).
 - [48] J. Gea-Banacloche, Y. Li, S. Jin, and M. Xiao, Phys. Rev. A **51**, 576 (1995).
 - [49] H. S. Moon, L. Lee, and J. B. Kim, J. Opt. Soc. Am. B **22**, 2529 (2005).
 - [50] A. Ray, Md. S. Ali, and A. Chakrabarti, Eur. Phys. J. D **67**, 78 (2013).
 - [51] H. S. Moon, L. Lee, and J. B. Kim, Opt. Exp. **16**, 12163 (2008).
 - [52] H. R. Noh and H. S. Moon, Phys. Rev. A **85**, 033817 (2012).
 - [53] M. O. Scully and M. S. Zubairy, Quantum Optics (Cambridge University Press, Cambridge, 1997).
 - [54] A. Miranowicz, M. Bartkowiak, X. Wang, Y. X. Liu, and F. Nori, Phys. Rev. A **82**, 013824 (2010).
 - [55] Z. G. Li, S. M. Fei, Z. X. Wang, and K. Wu, Phys. Rev. A **75**, 012311 (2007).